

# Clinical Cancer Research



## Polymeric Nanoparticle-Encapsulated Hedgehog Pathway Inhibitor HPI-1 (NanoHHI) Inhibits Systemic Metastases in an Orthotopic Model of Human Hepatocellular Carcinoma

Yang Xu, Venugopal Chenna, Chaoxin Hu, et al.

*Clin Cancer Res* 2012;18:1291-1302. Published OnlineFirst August 25, 2011.

**Updated version** Access the most recent version of this article at:  
doi:[10.1158/1078-0432.CCR-11-0950](https://doi.org/10.1158/1078-0432.CCR-11-0950)

**Supplementary Material** Access the most recent supplemental material at:  
<http://clincancerres.aacrjournals.org/content/suppl/2011/08/25/1078-0432.CCR-11-0950.DC1.html>

**Cited Articles** This article cites by 46 articles, 14 of which you can access for free at:  
<http://clincancerres.aacrjournals.org/content/18/5/1291.full.html#ref-list-1>

**Citing articles** This article has been cited by 2 HighWire-hosted articles. Access the articles at:  
<http://clincancerres.aacrjournals.org/content/18/5/1291.full.html#related-urls>

**E-mail alerts** [Sign up to receive free email-alerts](#) related to this article or journal.

**Reprints and Subscriptions** To order reprints of this article or to subscribe to the journal, contact the AACR Publications Department at [pubs@aacr.org](mailto:pubs@aacr.org).

**Permissions** To request permission to re-use all or part of this article, contact the AACR Publications Department at [permissions@aacr.org](mailto:permissions@aacr.org).

## Polymeric Nanoparticle-Encapsulated Hedgehog Pathway Inhibitor HPI-1 (NanoHHI) Inhibits Systemic Metastases in an Orthotopic Model of Human Hepatocellular Carcinoma

Yang Xu<sup>1,3</sup>, Venugopal Chenna<sup>3</sup>, Chaoxin Hu<sup>3</sup>, Hai-Xiang Sun<sup>1,2,3</sup>, Mehtab Khan<sup>3</sup>, Haibo Bai<sup>3</sup>, Xin-Rong Yang<sup>1</sup>, Qin-Feng Zhu<sup>2,3</sup>, Yun-Fan Sun<sup>1</sup>, Anirban Maitra<sup>3,4</sup>, Jia Fan<sup>1,2</sup>, and Robert A. Anders<sup>3</sup>

### Abstract

**Purpose:** To illustrate the prognostic significance of hedgehog (Hh) signaling in patients with hepatocellular carcinoma (HCC) and to evaluate the efficacy of a novel nanoparticle-encapsulated inhibitor of the Hh transcription factor, *Gli1* (NanoHHI) using *in vitro* and *in vivo* models of human HCCs.

**Experimental Design:** Patched1 (*Ptch1*) expression was detected in tumor tissue microarrays of 396 patients with HCC who underwent curative surgical resection during February 2000 to December 2002. Prognostic significance was assessed using Kaplan–Meier survival estimates and log-rank tests. The effects of NanoHHI alone and in combination with sorafenib were investigated on HCC cell lines. Primary HCC tumor growth and metastasis were examined *in vivo* using subcutaneous and orthotopic HCC xenografts in nude mice.

**Results:** Elevated expression of *Ptch1* in HCC tissues was significantly related to disease recurrence, as well as a shorter time to recurrence in patients with HCC. *In vitro*, NanoHHI significantly inhibited the proliferation and invasion of HCC cell lines. NanoHHI potently suppressed *in vivo* tumor growth of HCC xenografts in both subcutaneous and orthotopic milieus, and in contrast to sorafenib, resulted in significant attenuation of systemic metastases in the orthotopic setting. Furthermore, NanoHHI significantly decreased the population of CD133-expressing HCC cells, which have been implicated in tumor initiation and metastases.

**Conclusion:** Downstream Hh signaling has prognostic significance in patients with HCC as it predicts early recurrence. Gli inhibition through NanoHHI has profound tumor growth inhibition and antimetastatic effects in HCC models, which may provide a new strategy in the treatment of patients with HCC and prevention post-operative recurrence. *Clin Cancer Res*; 18(5); 1291–302. ©2011 AACR.

### Introduction

Hepatocellular carcinoma (HCC) is the third leading cause of cancer death worldwide, and the age-adjusted incidence rates have doubled over the past 2 decades

**Authors' Affiliations:** <sup>1</sup>Liver Cancer Institute, Zhong Shan Hospital and Shanghai Medical School, Key Laboratory for Carcinogenesis & Cancer Invasion, <sup>2</sup>Institute of Biomedical Sciences, Fudan University, The Chinese Ministry of Education, Shanghai, PR China; and The Sol Goldman Pancreatic Cancer Research Center, Departments of <sup>3</sup>Pathology and <sup>4</sup>Oncology, Johns Hopkins University School of Medicine, Baltimore, Maryland

**Note:** Supplementary data for this article are available at Clinical Cancer Research Online (<http://clincancerres.aacrjournals.org/>).

Y. Xu and V. Chenna contributed equally to the manuscript.

**Corresponding Authors:** Robert A. Anders, Department of Pathology, Division of Gastrointestinal and Liver Pathology, Room 346, CRB-II, Johns Hopkins University School of Medicine, 1550 Orleans St, Baltimore, MD 21231. Phone: 410-955-3511; Fax: 410-614-0671; E-mail: rander54@jhmi.edu and Jia Fan, Liver Cancer Institute, Fudan University, 136 Yi Xue Yuan Road, Shanghai 200032, PR China. Phone: 86-21-64037181; Fax: 86-21-64037181; E-mail: jiafan99@yahoo.com

doi: 10.1158/1078-0432.CCR-11-0950

©2011 American Association for Cancer Research.

(1, 2). Despite the advancement of therapeutic modalities including surgery and chemotherapy, the overall survival (OS) of patients with HCC remains unsatisfactory because of the high rate of recurrence and metastasis (3, 4). Sorafenib, a novel multikinase inhibitor, is the only targeting molecule which has recently been approved by U.S. Food and Drug Administration for the treatment of unresectable HCCs. Nevertheless, sorafenib only showed limited survival benefits in the patients with late-stage HCC and has no strong efficacy on tumor metastasis, which is the most common cause of death from HCC (5, 6). Hence, there is a pressing need for novel targeted pathway and alternative therapeutic modalities for treating HCCs.

The hedgehog (Hh) pathway is a major tissue growth regulator. The pathway is activated by the binding of mammalian Hh ligands (Sonic Hh, Indian Hh, and Desert Hh) to Patched (*Ptch1*) which relieves its inhibition on Smoothed (*Smo*) receptor, culminating in the nuclear localization of DNA-binding Gli transcription factors. These transcription factors lead to production of Hh target genes, such as *Ptch1* and *Gli1*, which also serve as convenient readouts of pathway activation. Together these components generally

### Translational Relevance

The hedgehog (Hh) pathway has been implicated in tumor initiation and metastases in hepatocellular carcinomas (HCC), and aberrant Hh activation predicts an adverse clinical outcome in patients undergoing curative HCC resection. Current small-molecule antagonists of Hh signaling bind to the Smoothened (*Smo*) receptor. However, secondary mutations of *Smo* and noncanonical activation of the Hh transcription factor Gli are emerging resistance mechanisms used by cancer cells to subvert the effectiveness of *Smo* antagonists. We have generated a polymeric nanoparticle-encapsulated formulation of a novel Gli inhibitor, HPI-1 (NanoHHI), which overcomes the systemic bioavailability pitfalls of the parental compound and blocks Hh signaling directly at the level of Gli function. *In vivo*, NanoHHI potently suppresses the development of HCC metastases in a lethal orthotopic model. Our findings have significant translational relevance in that recurrent metastatic disease represents the single most important basis for mortality following apparently curative HCC resection.

function to control tissue development of many tissue types (7–9). For example, in the fetus, this signaling pathway functions early in the endoderm to establish hepatic progenitor cells (10). However, Hh signaling appears to have a far more significant role in maintaining hepatic progenitors in the adult liver (11–13). The Hh pathway is activated during liver regeneration (13) and in response to chronic liver injury (11, 12, 14, 15).

Inappropriate activation of Hh pathway has been implicated in several gastrointestinal tumor types (16). Several studies have shown aberrant Hh signaling in human HCC tissues and cell lines. Hh signaling appears to be particularly active in the setting of chronic liver disease and might partially account for the common occurrence of HCC in the setting of chronic liver disease and cirrhosis (17, 18). Blockade of Hh signaling results in decreased proliferation and migration and an increase in apoptosis of human HCC cell lines (19–26). Other groups have implicated Hh transcriptional targets as critical to tumor progression and metastasis (21, 23).

Of the multiple small-molecule Hh inhibitors currently undergoing evaluation in clinical trials, all are *Smo* antagonists (27). However, there are 2 potential shortcomings for targeting *Smo* in human cancers. First is the recently described ability of tumors to secondarily acquire *Smo* mutations that can abrogate the ability of antagonists to bind to the heptahelical bundle of *Smo* protein (28–31). Second, *Smo*-independent pathways leading to Gli activation have been shown recently by Hanahan and colleagues (32). For these reasons, and evidence showing that RNA-mediated interference of *Gli1* causes apoptosis in human HCC cell lines but not in normal hepatocytes (20), we

evaluated a direct inhibitor of Gli which might provide improved therapeutic advantage in HCC.

Recently, 4 Hh pathway inhibitors (HPI 1–4) have been identified that block Hh signaling downstream of *Smo* (33). In particular, HPI-1 is a potent antagonist of Gli proteins (*Gli1* and 2) and also blocks Hh signaling in the setting of exogenous Gli expression. However, it might be difficult to translate these *in vitro* findings to *in vivo* studies as this inhibitor has poor systemic bioavailability. Its lipophilic nature and poor aqueous solubility make it difficult to deliver *in vivo*. We developed and characterized (34) a novel polymeric nanoparticle encapsulating HPI-1 (NanoHHI).

In this study, we first established the clinical significance of *Ptch1* expression in HCC, as a marker of downstream Hh activity. We show that *Ptch1* expression in patients undergoing curative HCC resection correlated with early recurrence and was a poor prognostic feature. Furthermore, we show that NanoHHI is effective at inhibiting the proliferation and motility of 2 human HCC cell lines *in vitro* and significantly inhibits subcutaneous tumor growth at least as effectively as the current standard-of-care chemotherapeutic agent, sorafenib. Notably, however, NanoHHI is remarkably more effectively than sorafenib at inhibiting metastasis in a lethal orthotopic model of human HCC. The ability to potently suppress systemic metastasis is likely attributed to the ability of NanoHHI to significantly downregulate CD133-expressing cells, which are implicated as tumor-initiating cells in HCCs. These studies provide early evidence of a nanoparticle-encapsulated agent that might be useful for chemotherapy in patients at high risk of HCC recurrence after curative surgical resection.

## Materials and Methods

### Patients and specimens

Tumor specimens used in tissue microarrays (TMA) were obtained from 396 patients with HCC who underwent surgical resection at the Liver Cancer Institute, Zhong Shan Hospital, Fudan University (Shanghai, PR China) from February 1, 2000, to December 1, 2002. Tumor specimens were taken from viable areas of the tumors and necrotic tissues were avoided. The inclusion criteria of all the patients in this study were as follows: (i) confirmed histopathologic diagnosis of HCC based on the WHO criteria (35); (ii) without any prior therapy; (iii) with an "intent-to-cure" surgical resection, which is defined as the complete resection of all tumor nodules and the margins being free of cancer by histologic examination (36); (iv) with suitable formalin-fixed, paraffin-embedded tissues; and (v) patients with demographic and clinicopathologic follow-up data. Tumor differentiation was defined according to the Edmondson grading system (37). Liver function was assessed by the Child–Pugh classification. Tumor staging was defined according to the sixth edition of tumor-node-metastasis (TNM) classification of Unio Internationale Contra Cancrum (UICC). The clinicopathologic characteristics of all the patients are summarized in Table 1. Ethical

**Table 1.** The clinical/pathologic characteristics of 396 cases of HCC

Clinical and pathologic indexes	N (%)
Age, y	
≤50	189 (47.7)
>50	207 (52.3)
Sex	
Female	50 (12.6)
Male	346 (87.4)
Liver cirrhosis	
No	99 (25.0)
Yes	297 (75.0)
Child–Pugh score	
A	217 (54.8)
B + C	179 (45.2)
HBsAg	
Negative	72 (18.2)
Positive	324 (81.8)
HCV	
Negative	386 (97.5)
Positive	10 (2.5)
GGT, U/L	
≤54	162 (40.9)
>54	234 (59.1)
ALT, U/L	
≤75	359 (90.7)
>75	37 (9.3)
AFP, ng/mL	
≤20	142 (35.9)
>20	254 (64.1)
Tumor encapsulation	
Complete	164 (41.4)
None	232 (58.6)
Tumor differentiation	
I–II	261 (65.9)
III–IV	135 (34.1)
Tumor size, cm	
≤5	230 (58.1)
>5	166 (41.9)
Tumor number	
Single	317 (80.1)
Multiple	79 (19.9)
Vascular invasion	
No	298 (75.3)
Yes	98 (24.7)
BCLC stage	
0 + A	169 (42.7)
B + C	227 (57.3)
TNM stage	
I	249 (62.9)
II–III	147 (37.1)
<i>Ptch1</i>	
Negative	295 (74.5)
Positive	101 (25.5)

Abbreviations: ALT, alanine aminotransferase; BCLC, Barcelona Clinic Liver Cancer; GGT,  $\gamma$ -glutamyl transferase.

approval for human subjects was obtained from the research ethics committee of Zhong Shan Hospital and the Johns Hopkins University (Baltimore, MD) Institutional Review Board.

#### Follow-up and tumor recurrences

Patients were followed up every 2 months during the first postoperative year and at least every 3 to 4 months afterward. Follow-up was obtained until March 30, 2010. All patients were prospectively monitored by serum  $\alpha$ -fetoprotein (AFP), abdominal ultrasonography, and radiography every 1 to 6 months in the postoperative period. A computed tomographic (CT) scan of the abdomen was conducted every 6 months. Bone scan or MRI was done if localized bone pain was reported. If recurrence was suspected, CT scan or MRI was conducted immediately. Most patients died from recurrence or metastasis or complicated liver cirrhosis. Patients with confirmed recurrence received further treatment, which followed the same protocol on the basis of the size, site, number of tumor nodules, and liver function. Briefly, if the recurrent tumor was localized, a second liver resection, radiofrequency ablation (RFA), or percutaneous ethanol injection (PEI) was conducted; if the recurrent tumor was multiple or diffuse, then transcatheter arterial chemoembolization (TACE) was the choice. External radiotherapy was given if lymph node or bone metastasis was found. Otherwise, symptomatic treatment was provided. OS was defined as the interval between surgery and death or the last observation taken. The data were censored at the last follow-up for living patients. Time to recurrence (TTR) was measured from the date of resection until the detection of recurrent tumor and data were censored for patients without signs of recurrence.

#### TMA and immunohistochemistry

TMA was constructed as previously described (38). Briefly, all the HCC and peritumoral liver tissues were reviewed by 2 histopathologists, and representative areas free from necrotic and hemorrhagic materials were premarked in the paraffin blocks. Two core biopsies of 1 mm in diameter were taken from the donor blocks and transferred to the recipient paraffin block at defined array positions. Two HCC and 2 respective peritumoral liver TMA blocks were constructed. Consecutive sections of 4- $\mu$ m thickness were taken on 3-aminopropyltriethoxysilane (APES)-coated slides (Shanghai Biochip Co., Ltd.). The rabbit polyclonal antibody for *Ptch1* was purchased from Santa Cruz Biotechnology, (No. sc-6149, diluted 1:100). Immunohistochemistry was carried out using a 2-step protocol (Novolink Polymer Detection System, Novocastra) as previously described (38, 39). Briefly, after microwave antigen retrieval, tissues were incubated with primary antibodies for 60 minutes at room temperature or overnight at 4°C. Following a 30-minute incubation with secondary antibody (A0545, Sigma), the sections were developed in 3,3'-diaminobenzidine (DAB) solution under microscopic observation and counterstained with hematoxylin. Negative control slides with the primary antibodies omitted were included in all assays.

### Evaluation of immunohistochemical variables

Immunohistochemical staining was assessed by 2 independent pathologists without knowledge of patient characteristics. Staining score of *Ptch1* was calculated according to the percentage of positive cells (cytoplasm) from 0 to 100, and the samples in the cohort were classified as negative when the scores ranged from 0 to 25 and positive when they fell between 26 and 100 based upon receiver operator characteristic (ROC) curve (Supplementary Fig. S1). All of the cases with different scorings were discussed under a multiheaded microscope until consensus was reached. The duplicate of spots for each tumor showed relative homogeneity for stained cell percentage and intensity. The higher score was considered as a final score in case of a difference between duplicate tissue cores.

### Drug formulations

NanoHHI was engineered as described (34). Sorafenib was purchased from Bayer Pharmaceutical Corporation and dissolved in sterile dimethyl sulfoxide and stored frozen under light-protected conditions at  $-20^{\circ}\text{C}$ .

### Cell culture

Huh7, HepG2, and MHCC97L (97L) human HCC cell lines were used in these studies. Huh7 and HepG2 were purchased from American Type Culture Collection. 97H and 97L were provided by Dr. Xin-Wei Wang from U.S. National Cancer Institute (Bethesda, MD) with the permission of Prof. Zhao-You Tang of Liver Cancer Institute, Fudan University. All the cell lines were routinely maintained at  $37^{\circ}\text{C}$  and 5%  $\text{CO}_2$  in Dulbecco's Modified Eagle's Media supplemented with 10% FBS and 1% penicillin/streptomycin.

### In vitro growth and Matrigel invasion assay

Cell proliferation was assessed using the MTT assay. Cells were seeded at a density of 2,000 cells per well and allowed to grow overnight. Huh7 and MHCC97L cells were treated with NanoHHI (40  $\mu\text{mol/L}$ ), sorafenib (10  $\mu\text{mol/L}$ ), or NanoHHI (40  $\mu\text{mol/L}$ ) + sorafenib (10  $\mu\text{mol/L}$ ). Cell viability was measured after 48 hours. Huh7 and MHCC97L cells were seeded onto a Matrigel-coated filter (No. 3458, Corning) containing NanoHHI (40  $\mu\text{mol/L}$ ), sorafenib (10  $\mu\text{mol/L}$ ), or NanoHHI (40  $\mu\text{mol/L}$ ) + sorafenib (10  $\mu\text{mol/L}$ ) for the cell invasion assay and incubated for 8 hours at  $37^{\circ}\text{C}$ . The cells that actively migrated to the lower surface of the filters were stained and quantified. All assays were conducted in triplicate.

### In vivo preclinical studies on NanoHHI efficacy

Male athymic BALB/c *nu/nu* mice, 4- to 6-week-old, were purchased from Jackson Laboratory. All studies on mice were conducted in accordance with the NIH "Guide for the Care and Use of Laboratory Animals" (Bethesda, MD). The study protocol was approved by Medical Experimental Animal Care Committee of Johns Hopkins University. Subcutaneous and orthotopic HCC models were estab-

lished as described before (25). Briefly, approximately,  $5 \times 10^6$  Huh7 cells in 0.2 mL culture medium were injected subcutaneously into the right flank of athymic mice, which were then observed daily for signs of tumor development. Once the subcutaneous tumor reached 1 cm in diameter, it was removed and freshly minced into pieces about  $2 \text{ mm}^3$ , which were implanted into the liver of athymic mice, using the method as described previously (25). The subcutaneous and orthotopic models were administered drugs beginning at day 7 following tumor cell injection or tumor implantation. Twenty subcutaneous and 20 orthotopic tumor mice were randomly assigned to 4 experimental groups. The 4 experimental groups were as follows: untreated control group, NanoHHI (30 mg/kg, intraperitoneally, twice a day for 4 weeks), sorafenib (20 mg/kg, orally taken by gavage in 1% dimethyl sulfoxide, twice a day for 4 weeks) treatment group, and NanoHHI-combined sorafenib treatment group (administered by using the same schedule for each drug as described for the single treatment). All control mice received an equal volume of carrier solution by gavage and injection, respectively. The mice were sacrificed 4 weeks after treatment. At necropsy, tumor volume was measured for largest (*a*) and smallest (*b*) diameters, and the tumor volume was calculated as  $V = a \times b^2/2$ . Tumors were either homogenized for Western blot analysis and quantitative reverse transcriptase PCR (qRT-PCR) or fixed in paraformaldehyde for 24 hours, and paraffin sections were used for immunohistochemical staining. Metastatic implants in abdominal and thoracic organs and surfaces were determined at the time of necropsy by serial sectioning of organs coupled with gross and histologic inspection. Paraffin blocks of 10% buffered formalin-fixed samples of lung were prepared and serial sections were cut at 4  $\mu\text{m}$  and stained with hematoxylin and eosin to determine the presence of lung metastases.

### qRT-PCR, Western blot analysis, and flow cytometry

Total RNA was prepared using TRIzol (Invitrogen), and then cDNA was synthesized using the Superscript First-Strand Synthesis System (Invitrogen). Real-time qRT-PCR amplification for human *Gli1* (hGli1) and *Gli2* (hGli2) and murine *Gli1* (*mGli1*) and *Gli2* (*mGli2*) was carried out with TaqMan Fast Universal PCR Master Mix (Applied Biosystem). The qRT-PCR was carried out with an Applied Biosystem Step One Plus system using  $\beta$ -actin (assay ID Mm01205647, reference sequence ID NM\_001101.2) as housekeeping control. The assay ID for *mGli1* is 00494645\_m1 and the reference sequence is NM\_010296.2. Relative mRNA levels were calculated on the basis of the  $2^{-\Delta\Delta C_t}$  method. Anti-human CD133-PE antibody (No. 130-080-801, MACS) was used for CD133 immunofluorescent detection by flow cytometry. Isotope-matched mouse immunoglobulin (No. 130-092-212, MACS) was incorporated as controls. Cells were incubated in PBS containing 2% FBS and 0.1% sodium azide with fluorescence-conjugated primary antibody. Samples were analyzed using a FACSCalibur flow cytometer and CellQuest software (BD Biosciences).

### Statistical analysis

Statistical analyses were conducted by SPSS 15.0 for Windows (SPSS). Cumulative survival time was calculated by the Kaplan–Meier method and analyzed by the log-rank test. Univariate and multivariate analyses were based on the Cox proportional hazards regression model. The  $\chi^2$  test, Fisher's exact probability test, and Student *t* test were used for comparison between groups.  $P < 0.05$  was considered statistically significant.

### Results

#### Expression of *Ptch1* and relevance to prognostic factors

There are reports of Hh signaling components expressed in human HCC tissues; however, these results have not been linked to clinical outcome (21, 40). We examined *Ptch1* expression, as a downstream marker of Hh activation, using immunohistochemical staining of a TMA constructed from 396 patients who had undergone HCC resection with curative intent. The clinical and pathologic characteristics

of this patient cohort revealed that 207 (52%) patients were older than 50 years, 346 (87.4%) were men with 324 (81.8%) being infected with chronic hepatitis B (Table 1). *Ptch1* expression was detected in 101 (25.5%) HCC tumor samples, whereas only 33 (8.3%) of the nontumor tissue yielded positive *Ptch1* labeling (Table 1). The expression of *Ptch1* was significantly elevated in tumor tissue samples compared with the nontumor counterparts ( $P < 0.01$ ). Staining was relatively homogenous within a neoplasm, excluding necrotic, hemorrhagic, and fibrotic regions. Compared with control staining, *Ptch1* was detected predominantly in the cytoplasm of tumor cells and was also present to a lesser extent at the cell membrane (Fig. 1A–D). *Ptch1* expression in tumor tissue correlated with patient age of presentation, tumor encapsulation, and recurrence (Table 2). For the whole study population, the 5-year OS and TTR rates were 53.4% and 46.3%, respectively. On univariate analysis, significant poor predictors of OS included serum hepatitis B surface antigen; Child–Pugh score; serum  $\gamma$ -glutamyl transpeptidase and AFP; tumor

**Figure 1.** *Ptch1* expression in patients with HCC. Representative images from TMAs containing 396 patients with HCC. A, hematoxylin and eosin (H&E) and immunohistochemical staining of HCC with (B) control IgG and (C and D) anti-*Ptch1* antibody. E, mean relapse time for each patient was calculated and compared between HCCs that do and do not express *Ptch1*. F, Kaplan–Meier analysis showed that high *Ptch1* expressing HCCs correlate with a significantly higher rate of tumor recurrence. These trends are most marked in patients with (G) advanced stage (TNM II–III) cancers and (H) well-differentiated (Edmondson grade I–II) histologic grade (D). \*\*,  $P < 0.05$ .

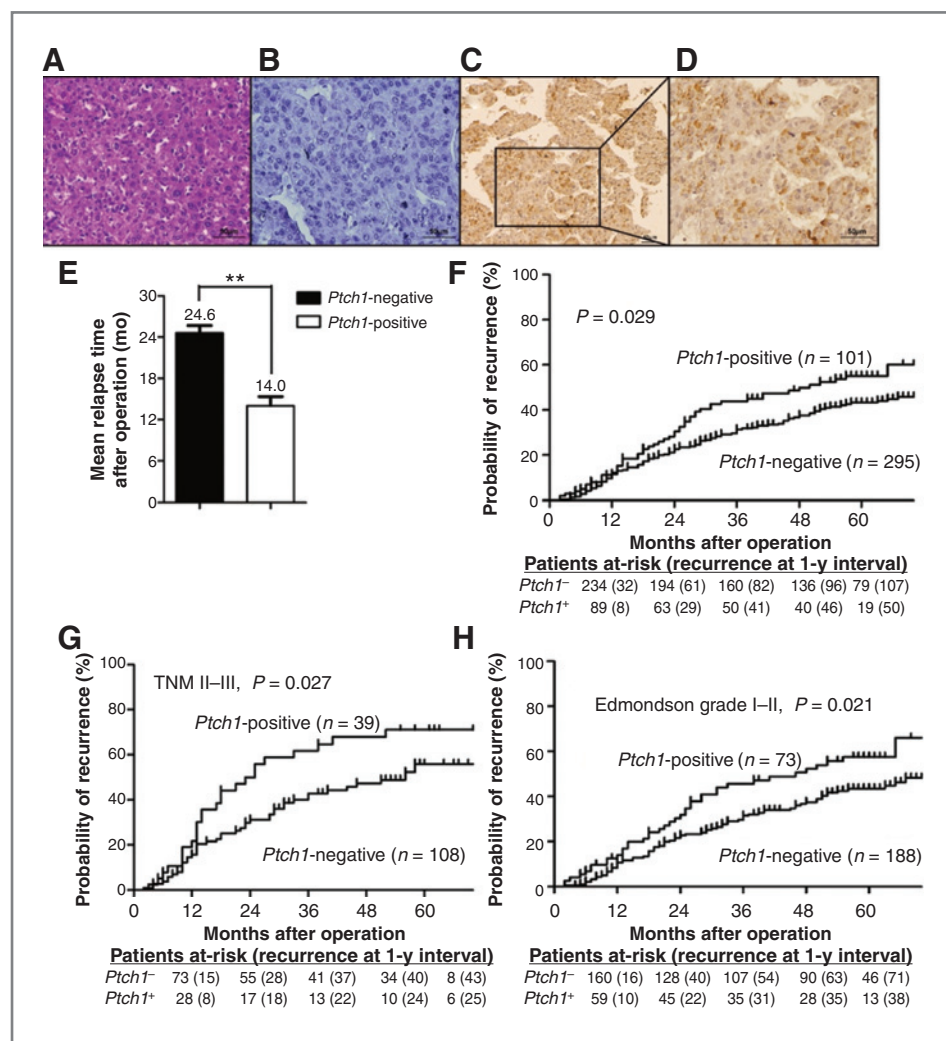


**Table 2.** Univariate analyses of factors associated with survival and recurrence (N = 396)

Variables	OS		RFS	
	HR (95% CI)	P	HR (95% CI)	P
Sex (male vs. female)	1.12 (0.72–1.74)	0.631	0.98 (0.62–1.55)	0.920
Age, y (>50 vs. ≤50)	0.86 (0.65–1.14)	0.293	1.07 (0.78–1.45)	0.682
HBsAg (positive vs. negative)	1.73 (1.14–2.64)	0.010	1.08 (0.72–1.60)	0.722
HCV (positive vs. negative)	0.90 (0.37–2.20)	0.822	1.13 (0.46–2.76)	0.787
Child–Pugh score (B + C vs. A)	1.31 (1.02–1.68)	0.033	0.89 (0.67–1.18)	0.425
Liver cirrhosis (yes vs. no)	0.88 (0.63–1.23)	0.448	1.07 (0.75–1.51)	0.715
GGT, U/L (>54 vs. ≤54)	1.62 (1.20–2.18)	0.001	1.33 (0.97–1.82)	0.078
ALT, U/L (>75 vs. ≤75)	0.98 (0.60–1.62)	0.944	0.74 (0.41–1.34)	0.318
AFP, ng/mL (>20 vs. ≤20)	1.82 (1.32–2.50)	0.000	1.26 (0.91–1.75)	0.158
Tumor differentiation (III–IV vs. I–II)	1.14 (0.85–1.53)	0.376	0.88 (0.63–1.23)	0.441
Tumor encapsulation (none vs. complete)	0.59 (0.45–0.78)	0.000	0.88 (0.65–1.21)	0.441
Tumor size, cm (>5 vs. ≤5)	1.85 (1.30–2.65)	0.001	0.88 (0.59–1.31)	0.523
Tumor number (multiple vs. single)	2.30 (1.68–3.15)	0.000	2.10 (1.47–3.00)	0.000
Vascular invasion (yes vs. no)	1.97 (1.45–2.67)	0.000	1.51 (1.06–2.14)	0.023
TNM stage (II + III vs. I)	2.34 (1.76–3.11)	0.000	1.82 (1.33–2.50)	0.000
BCLC stage (B + C vs. 0 + A)	1.83 (1.36–2.47)	0.000	1.25 (0.91–1.70)	0.166
<i>Ptch1</i> (positive vs. negative)	1.06 (0.77–1.46)	0.716	1.48 (1.07–2.06)	0.019

NOTE: Univariate analysis, Cox proportional hazards regression model.

Abbreviations: ALT, alanine aminotransferase; BCLC, Barcelona Clinic Liver Cancer; CI, confidence interval; GGT,  $\gamma$ -glutamyl transpeptidase; RFS, relapse-free survival; TACE, transcatheter arterial chemoembolization.

encapsulation, size and number; vascular invasion; and TNM and Barcelona Clinic Liver Cancer (BCLC) stage (Table 3). Significant factors associated with TTR were the number of tumors, vascular invasion, advanced TNM stage, and *Ptch1* expression. On multivariate analysis, AFP and tumor size were independent factors associated with

OS. *Ptch1* expression was an independent predictive factor of TTR (Table 4). Patients with *Ptch1*-expressing tumors had significantly reduced mean time to relapse compared with those without *Ptch1* expression (5-year TTR rate, 43.7% vs. 54.3%,  $P = 0.029$ ; Fig. 1E and F). The significant prognostic role of *Ptch1* was also apparent in patients with late-stage

**Table 3.** Multivariate analyses of factors associated with OS and RFS (N = 396)

Variables	OS		RFS	
	HR (95% CI)	P	HR (95% CI)	P
HBsAg (positive vs. negative)	1.51 (0.98–2.33)	0.063	n.a.	
Child–Pugh score (B + C vs. A)	1.17 (0.91–1.51)	0.218	n.a.	
GGT, U/L (>54 vs. ≤54)	1.35 (0.99–1.83)	0.059	n.a.	
AFP, ng/mL (>20 vs. ≤20)	1.49 (1.08–2.07)	0.015	n.a.	
Tumor encapsulation (none vs. complete)	0.78 (0.58–1.05)	0.097	n.a.	
Tumor size, cm (>5 vs. ≤5)	2.08 (1.21–3.55)	0.008	n.a.	
Tumor number (multiple vs. single)	1.40 (0.81–2.40)	0.229	2.05 (1.42–2.97)	0.000
Vascular invasion (yes vs. no)	1.20 (0.69–2.08)	0.514	1.00 (0.72–1.39)	0.994
TNM stage (II + III vs. I)	1.76 (0.87–3.56)	0.117	1.39 (0.96–2.00)	0.078
BCLC stage (B + C vs. 0 + A)	0.64 (0.37–1.10)	0.103	n.a.	
<i>Ptch1</i> (positive vs. negative)	n.a.		1.53 (1.09–2.14)	0.013

NOTE: Multivariate analysis, Cox proportional hazards regression model. The clinicopathologic variables were adopted for their prognostic significance by univariate analyses.

Abbreviations: BCLC, Barcelona Clinic Liver Cancer; CI, confidence interval; GGT,  $\gamma$ -glutamyl transpeptidase; n.a., not applicable; RFS, relapse-free survival.

**Table 4.** Correlation between *Ptch1* and clinicopathologic characteristics

Clinicopathologic indexes	<i>Ptch1</i> <sup>-</sup> (n = 295)	<i>Ptch1</i> <sup>+</sup> (n = 101)	P
Sex			
Female	38	12	0.864
Male	257	89	
Age, y			
≤52	150	39	0.038
>52	145	62	
HBsAg			
Negative	54	18	1.000
Positive	241	83	
HCV			
Negative	288	98	0.720
Positive	7	3	
Liver cirrhosis			
No	221	76	1.000
Yes	74	25	
ALT, U/L			
≤75	264	95	0.234
>75	31	6	
Child–Pugh score			
A	158	59	0.419
B + C	137	42	
GGT, U/L			
≤54	119	43	0.726
>54	176	58	
AFP, ng/mL			
≤20	104	38	0.719
>20	191	63	
Tumor encapsulation			
Complete	132	32	0.026
No	163	69	
Tumor size, cm			
≤5	170	60	0.816
>5	125	41	
Tumor number			
Single	237	80	0.885
Multiple	58	21	
Vascular invasion			
No	222	76	1.000
Yes	73	25	
TNM stage			
I	187	62	0.722
II–III	108	39	
Tumor differentiation			
I–II	188	73	0.144
III–IV	107	28	
BCLC stage			
0 + 1	129	40	0.487
2 + 3 + 4	166	61	
Recurrence			
No	184	49	0.019
Yes	111	52	

NOTE: Fisher's exact tests;  $\chi^2$  tests for all the other analyses. Abbreviations: ALT, alanine aminotransferase; BCLC, Barcelona Clinic Liver Cancer; GGT,  $\gamma$ -glutamyl transferase.

HCC (TNM II–III,  $P = 0.027$ ) and the patients with well-differentiated tumors (Edmondson grade I–II,  $P = 0.021$ ; Fig. 1G and H). These series of data show that downstream Hh signaling appears to correlate with HCC recurrence.

#### NanoHHI inhibits HCC cell proliferation and invasion *in vitro*

We wanted to determine whether suppressing downstream Hh activity with a potent Gli inhibitor could inhibit the *in vitro* growth of HCC cell lines (34). We found that NanoHHI significantly ( $P < 0.029$ ) suppressed Huh7 cell growth compared with vehicle control and to a comparable degree as sorafenib (Fig. 2A). In another human HCC cell line, MHCC97L, sorafenib significantly suppressed *in vitro* growth, whereas NanoHHI showed some growth suppression, but this was not statistically different than control ( $P > 0.05$ ; Fig. 2A). Because downstream Hh activity is associated with HCC invasion (21, 23), we next measured the ability of NanoHHI to inhibit invasion. We found that NanoHHI significantly suppressed the ability of both Huh7 and MHCC97L cells to invade into Matrigel as compared with vehicle treatment (Fig. 2B and C). Similarly, sorafenib significantly inhibited HCC invasion *in vitro* in both cell lines, with a minor but not statistically significant additive effect when cells were treated with both NanoHHI and sorafenib (Fig. 2B and C).

#### NanoHHI potently inhibits HCC growth and metastasis *in vivo*

One week after subcutaneous injection of the Huh7 cell line into athymic mice, they received treatment with vehicle, NanoHHI (30 mg/kg twice daily intraperitoneally), sorafenib (20 mg/kg twice daily, *per os*), or both. After 4 weeks of treatments, tumor tissues were collected. No demonstrable adverse effects such as body weight loss were observed in any the groups. The weight of the subcutaneous xenografts in the mice in all 3 treatment groups were significantly decreased compared with those in vehicle group ( $P < 0.05$ ; Fig. 3A). As expected, transcript analysis in the Huh7 cell line showing NanoHHI treatment significantly suppresses human *Gli1* and *Gli2* (hGli1, hGli2) consistent with the well-characterized Hh inhibitory role of the parental molecule (33). Sorafenib had little effect on hGli1 but did show a decrease in hGli2 expression (Fig. 3C). The treated xenografts showed significant reduction in hGli1 and hGli2 as well as *mGli1* and *mGli2* levels (Fig. 3D and E). Of note, there was no significant decrease in hGli1, hGli2 or *mGli1*, *mGli2* expression in the sorafenib-treated xenografts. In tumors receiving combination therapy, there was significant suppression of hGli1 and *mGli2*.

For orthotopic xenograft studies, a sterile 2 mm<sup>3</sup> piece of subcutaneous Huh7 tumor was implanted orthotopically into athymic nude male mice. After 1 week of implantation, treatment with NanoHHI (30 mg/kg twice daily), sorafenib (20 mg/kg), or both agents was initiated for a period of 4 weeks. At the end of the treatment, orthotopic liver xenografts were harvested. At the time of

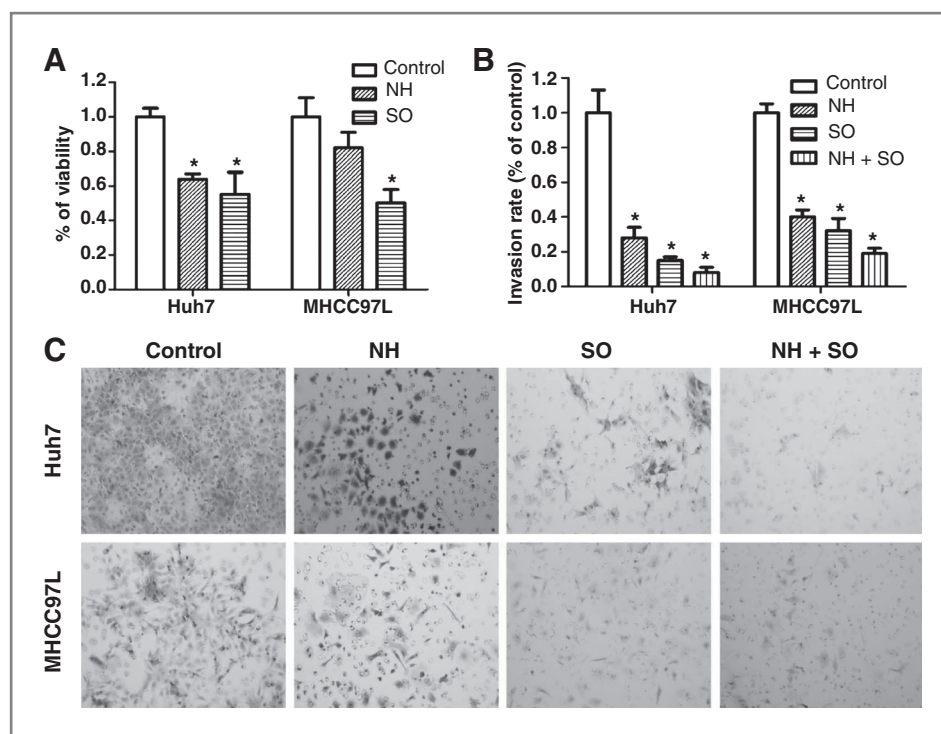


**Figure 2.** NanoHhI inhibits HCC growth and invasion *in vitro*. A, Huh7 and MHCC97L cell lines were treated with NanoHhI (NH; 40  $\mu\text{mol/L}$ ), sorafenib (SO; 10  $\mu\text{mol/L}$ ) for 48 hours and viability was determined with MTT assay. B, Huh7 and MHCC97L cells were seeded onto a Matrigel-coated filter containing NH (40  $\mu\text{mol/L}$ ), SO (10  $\mu\text{mol/L}$ ), and NH (40  $\mu\text{mol/L}$ ) + SO (10  $\mu\text{mol/L}$ ) for the cell invasion assay and incubated for 8 hours. The cells that actively migrated to the lower surface of the filters were stained (C) and quantified and reported as percentage of control. \*,  $P < 0.05$ .

harvest, grossly evident peritoneal metastases were recorded and liver, lung, and lymph nodes were collected for histologic examination. A total of 16 tumor metastasis involving the liver, lung, peritoneum, mesentery, diaphragm, and lymph nodes were found in all (5 of 5 mice) of the mice of control group and 15 metastases were found in 3 of 5 mice in the sorafenib group (Fig. 3B). Remarkably, only 2 metastases were found in 2 mice of NanoHhI group (Fig. 3B). These were satellite, intrahepatic spread of tumors that were physically discontinuous from the initial tumor implant and not distant metastasis. Similarly, only 3 total metastatic lesions were found in the mice treated with both NanoHhI and sorafenib (Fig. 3B). Taken as a whole, these data show that NanoHhI treatment potently suppresses HCC metastases.

#### NanoHhI decreases the population of CD133-positive HCC cells

To begin to understand that how NanoHhI could suppress metastatic spread, we examined CD133 expression as it has been linked to Hh signaling and identifies a subpopulation of cancer-initiating cells which could account for formation of metastasis (19). First, we found that NanoHhI treatment significantly downregulated CD133 mRNA in the orthotopic liver tumors harvested 4 weeks after the indicated treatments compared with control treatment ( $P < 0.05$ ; Fig. 3F). Sorafenib and combination treatment also showed a decrease in CD133. Because CD133 expression is not unique to cancer-initiating cells (19, 41, 42), we also looked at these treatments on Huh7 cells *in vitro*. We saw that sorafenib treatment did not show a significant inhibi-

tion of CD133, whereas NanoHhI and combination treatment with both agents did significantly downregulate CD133 transcription (Fig. 3G). This was also true after extended sorafenib treatment period at more than one dose (Supplementary Fig. S2). Flow cytometric analysis showed that NanoHhI significantly decreased the population of CD133-positive cells compared with control (4.5% vs. 21.1%,  $P < 0.01$ ; Fig. 3I). Again, sorafenib showed a trend to decrease CD133 surface expression but it was not statistically significant (19, 41–43). As expected, sorafenib significantly decreased the expression of phospho-extracellular signal-regulated kinase *in vitro* and *in vivo* compared with control treatment as determined by Western blot analysis (Fig. 3H). Combination treatment of Huh7 cells with both NanoHhI and sorafenib showed a similar decrease as was seen with sorafenib alone. Collectively, these data support that inhibiting Hh with NanoHhI suppresses CD133-positive HCC tumor-initiating cells and leads to the observed reduction in systemic *in vivo* metastases.

#### Discussion

Survival for HCC remains dismal with surgical resection offering the best hope for cure. However, recurrent HCC occurs in a staggering 50% to 80% of patients with most occurring in the first 2 years (1, 3). It is not clear if early recurrence occurs due to residual microscopic foci of malignant cells undetectable at the time of surgery, dissemination during surgery, or formation of *de novo* tumors (44). Regardless, there is significant need to target pathways responsible for HCC

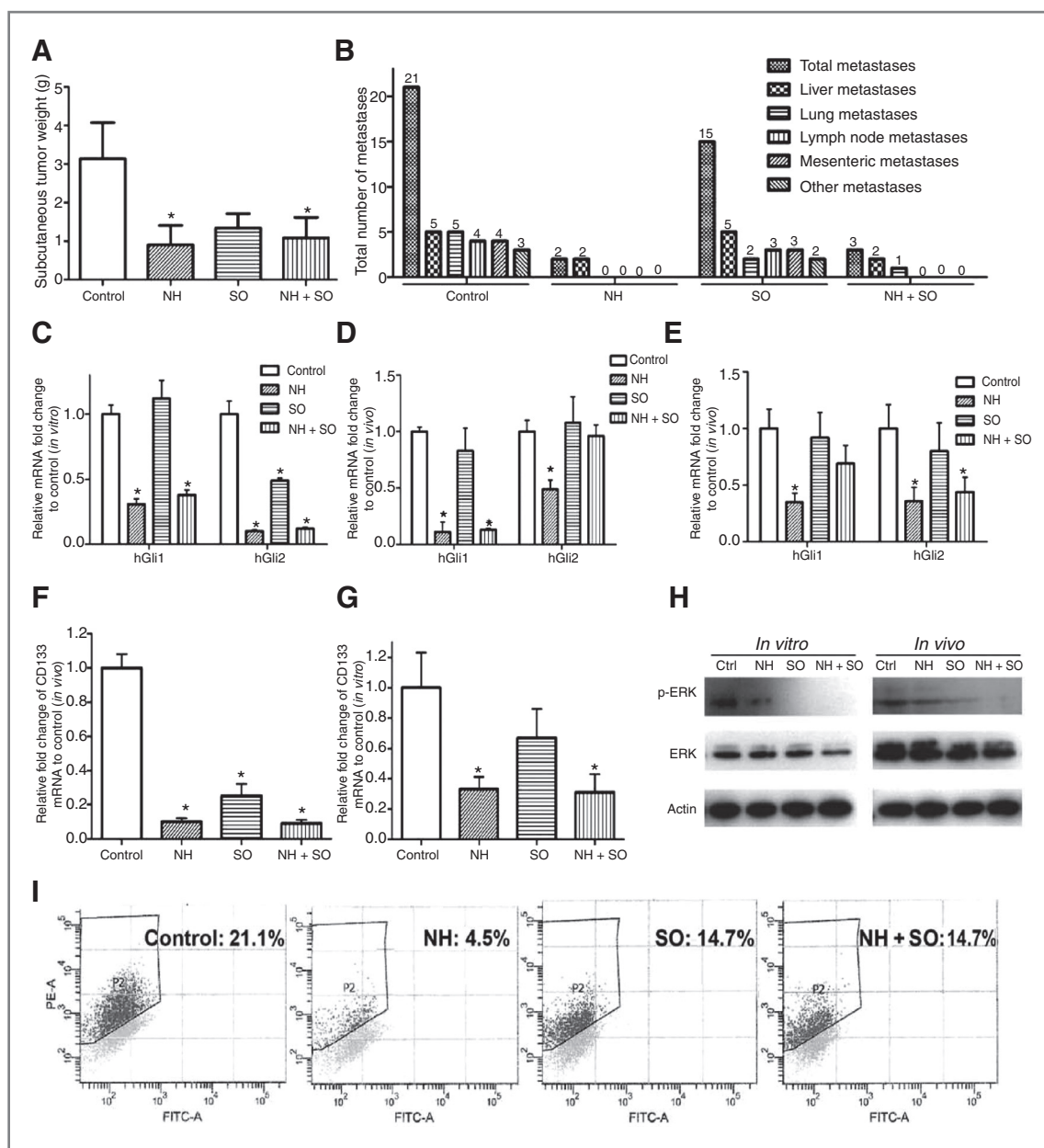


**Figure 3.** NanoHHLI inhibits HCC growth and *Gli1* and *Gli2* expressions, potently suppresses metastasis, and decreases CD133 expression. **A**, after 28 days of NanoHHLI (NH; 35 mg/kg, intraperitoneally, twice a day) and/or sorafenib (SO; 20 mg/kg, oral gavage, twice a day) treatments, the weight of subcutaneous tumors (Huh7) in nude mice was significantly decreased in the NH and combined NH + SO treatment groups compared with those in control group. **B**, an 8 mm<sup>3</sup> Huh7 subcutaneous tumor fragment was implanted into each mouse liver, and after 7 days, mice were randomized to 1 of 4 experimental groups. After 28 days of NH (35 mg/kg, intraperitoneally, twice a day) and/or SO (20 mg/kg, oral gavage, twice a day) treatments, metastatic implants were counted in the peritoneum, liver, thorax, and lungs by gross and histologic examination. Huh7 multiple tumor metastases were found in all the mice of control group whereas NH significantly inhibited tumor metastasis *in vivo*. **C**, Huh7 cells were untreated (control) or treated with NH (40 μmol/L), SO (10 μmol/L), and NH (40 μmol/L) + SO (10 μmol/L), and human *Gli1* and *Gli2* mRNA expressions were determined by qRT-PCR after 48 hours (\*, *P* < 0.05). **D**, human *Gli1* and *Gli2* or E, murine *Gli1* and *Gli2* mRNA expressions in orthotopic tumors after 28 days of NH and/or SO treatments *in vivo* were determined by qRT-PCR. Expression levels in the treatment groups are expressed relative to untreated (control) mRNA expression (\*, *P* < 0.05). **F**, CD133 mRNA expression in Huh7 orthotopic tumors was determined by qRT-PCR in the indicated treatment groups. Untreated (Control), NH (35 mg/kg, intraperitoneally, twice a day), SO (20 mg/kg, oral gavage, twice a day), and NH + SO (\*, *P* < 0.05). **G**, Huh7 cells were untreated (Control) or treated with NH (40 μmol/L), SO (10 μmol/L), and NH (40 μmol/L) + SO (10 μmol/L), and CD133 mRNA expression was determined by qRT-PCR (\*, *P* < 0.01). Data expressed relative to the control treatment where expression was set to 1.0. **H**, extracellular signal-regulated kinase (ERK) and p-ERK expressions were determined with Western blot analysis after treatment with NH and/or SO *in vitro* and *in vivo*. Ctrl, control. **I**, flow cytometric analysis showed that NH significantly decreased the population of CD133-positive cells *in vitro*. All *in vitro* assays were conducted in triplicate, and the mean ± SDs are presented. \*, *P* < 0.05, all compared with control. FITC, fluorescein isothiocyanate; PE, phycoerythrin.

recurrence and develop therapies specifically aimed at preventing or delaying HCC recurrence and metastasis.

Activity of Hh signaling in the liver has been documented. Hh ligands are significantly expressed in diseased human liver tissue and cirrhosis (17, 18). This is particularly important as a majority of HCCs occur in the setting of cirrhosis. Increased Hh activity has been shown in HCC (19–26). We found that increased *Ptch1* expression in HCC was a significant poor prognostic factor for patients undergoing curative resection. This was also true in patients with more advanced disease. Interestingly, at least 2 other studies have documented increased Hh activity and an association with invasion (21, 23). These data taken in the context of other publications provide rationale for suppressing Gli activity in treating HCCs and particularly in preventing the vexing problem of postsurgical recurrence.

Current Hh signaling suppressive agents target at the level of *Smo*. However, this might not be the ideal target in HCCs. Rare primary *Smo* mutations have also been reported in HCC, although the significance of these mutations to antagonist binding is unknown (26). TGF- $\beta$  is capable of *Smo*-independent stimulation of *Gli1* (32). TGF- $\beta$  activity is particularly important in HCCs as the activity of this pathway correlates with poor clinical outcome (26, 31, 45). Second, malignancies develop secondary, nononcogenic *Smo* mutations that make cells resistant to *Smo* antagonists (28–30). Mutation of *Smo* has been specifically reported in HCCs (26). Targeting *Ptch1* might not be ideal either because polymorphism in *Ptch1* has been linked to HCC differentiation or the functional significance of these polymorphisms is not clear (40). Finally, the downstream Hh target, *GLI1*, is amplified in cancers but has not been specifically described in HCCs (28, 29). For these reasons, we aimed to suppress the downstream Hh target *Gli1*.

To suppress Gli activity, we turned to HPI-1, a molecule that Hyman and colleagues uncovered in a screen of small molecules aimed at suppressing Hh activity downstream of *Smo* (33). However, the native HPI-1 molecule is lipophilic and not water soluble which will likely translate into poor bioavailability. Therefore, we used a polymeric nanoparticle-encapsulated formulation (NanoHHI) which has been developed as a nontoxic and safe Gli inhibitor for *in vivo* studies (34).

We found that NanoHHI significantly inhibited HCC proliferation and invasion to a similar degree as sorafenib *in vitro*. A striking difference was seen *in vivo*, with NanoHHI potently suppressing metastatic spread whereas sorafenib had practically no effect. A recent report addressed a similar question (46). Like the study of Feng and colleagues, we both show that sorafenib decreases tumor growth *in vivo*.

However, they show a much more significant effect of sorafenib on tumor metastasis than we do. A key difference between these studies is their use of partial hepatectomy to remove the primary tumor before initiating sorafenib therapy. These therapies need not be mutually exclusive as they target different pathways. Combination therapy with sorafenib and NanoHHI showed comparable rates of metastasis as NanoHHI alone (Fig. 2B), with the combination of agents still suppressing *Gli1* and *Gli2* derived from the tumor cells (Fig. 3D). This is not entirely surprising as it is likely that multiple pathways contribute to HCC metastasis. Together this suggests that Hh activity could account for a bad prognosis and increased tumor dissemination and, taken with our *in vivo* metastasis data, suggests that suppressing Gli activity might improve the dismal recurrence rates in HCCs.

The possible mechanisms of the antimetastatic efficacy of NanoHHI include (i) Inhibition of Hh signaling pathway which has been confirmed as one of the important pathways of cancer-initiating/stem cell in our previous studies (23) and (ii) NanoHHI significantly decreased the population of CD133-positive HCC cells, which has been considered as HCC cancer-initiating/stem cell and the source of metastasis and recurrence of HCCs. A recent study highlighted the link between Hh activity and CD133 and found that well-differentiated tumors harbored a CD133-expressing subpopulation that was more tumorigenic hence requiring less CD133-positive cells to initiate HCCs when injected in the kidney capsule (19). This population of HCCs provides a reservoir of cells that can self-renew, undergo asymmetric division, and might be partially responsible for recurrence after ablative surgery. Furthermore, the CD133-positive population of cells has also been linked to vascular invasion and resistance to chemoradiotherapy (41, 47).

#### Disclosure of Potential Conflicts of Interest

No potential conflicts of interest were disclosed.

#### Grant Support

This study was supported by grants from National Natural Science Foundation of China (No. 81030038, 81071661, 30873039); Shanghai Rising-Star Follow-up Program Funds (No. 10QH1400500); National Key Sci-Tech Special Project of Infectious Diseases (No. 2008ZX10002-022); NIH R01DK080736 (R.A. Anders); R01DK081417 (R.A. Anders); Michael Rolfe Foundation for Pancreatic Cancer Research (A. Maitra and R.A. Anders); U54CA151838 (A. Maitra), and the Flight Attendants Medical Research Institute (A. Maitra).

The costs of publication of this article were defrayed in part by the payment of page charges. This article must therefore be hereby marked *advertisement* in accordance with 18 U.S.C. Section 1734 solely to indicate this fact.

Received April 20, 2011; revised July 15, 2011; accepted August 10, 2011; published OnlineFirst August 25, 2011.

#### References

- Llovet JM, Burroughs A, Bruix J. Hepatocellular carcinoma. *Lancet* 2003;362:1907–17.
- Seeff LB. Introduction: The burden of hepatocellular carcinoma. *Gastroenterology* 2004;127:S1–4.
- Lau WY, Lai EC. Hepatocellular carcinoma: current management and recent advances. *Hepatobiliary Pancreat Dis Int* 2008;7:237–57.
- Pawlik TM. Debate: Resection for early hepatocellular carcinoma. *J Gastrointest Surg* 2009;13:1026–8.

5. Llovet JM, Ricci S, Mazzaferro V, Hilgard P, Gane E, Blanc JF, et al. Sorafenib in advanced hepatocellular carcinoma. *N Engl J Med* 2008;359:378–90.
6. Yau T, Chan P, Ng KK, Chok SH, Cheung TT, Fan ST, et al. Phase 2 open-label study of single-agent sorafenib in treating advanced hepatocellular carcinoma in a hepatitis B-endemic Asian population: presence of lung metastasis predicts poor response. *Cancer* 2009;115:428–36.
7. Beachy PA, Karhadkar SS, Berman DM. Tissue repair and stem cell renewal in carcinogenesis. *Nature* 2004;432:324–31.
8. Omenetti A, Diehl AM. The adventures of sonic hedgehog in development and repair. II. Sonic hedgehog and liver development, inflammation, and cancer. *Am J Physiol Gastrointest Liver Physiol* 2008;294:G595–8.
9. Hooper JE, Scott MP. Communicating with Hedgehogs. *Nat Rev Mol Cell Biol* 2005;6:306–17.
10. Deutsch G, Jung J, Zheng M, Lora J, Zaret KS. A bipotential precursor population for pancreas and liver within the embryonic endoderm. *Development* 2001;128:871–81.
11. Sicklick JK, Li YX, Choi SS, Qi Y, Chen W, Bustamante M, et al. Role for hedgehog signaling in hepatic stellate cell activation and viability. *Lab Invest* 2005;85:1368–80.
12. Sicklick JK, Li YX, Melhem A, Schmelzer E, Zdanowicz M, Huang J, et al. Hedgehog signaling maintains resident hepatic progenitors throughout life. *Am J Physiol Gastrointest Liver Physiol* 2006;290:G859–70.
13. Ochoa B, Syn WK, Delgado I, Karaca GF, Jung Y, Wang J, et al. Hedgehog signaling is critical for normal liver regeneration after partial hepatectomy in mice. *Hepatology* 2010;51:1712–23.
14. Choi SS, Omenetti A, Witek RP, Moylan CA, Syn WK, Jung Y, et al. Hedgehog pathway activation and epithelial-to-mesenchymal transitions during myofibroblastic transformation of rat hepatic cells in culture and cirrhosis. *Am J Physiol Gastrointest Liver Physiol* 2009;297:G1093–106.
15. Omenetti A, Yang L, Li YX, McCall SJ, Jung Y, Sicklick JK, et al. Hedgehog-mediated mesenchymal-epithelial interactions modulate hepatic response to bile duct ligation. *Lab Invest* 2007;87:499–514.
16. Berman DM, Karhadkar SS, Maitra A, Montes De Oca R, Gerstenblith MR, Briggs K, et al. Widespread requirement for Hedgehog ligand stimulation in growth of digestive tract tumours. *Nature* 2003;425:846–51.
17. Pereira Tde A, Witek RP, Syn WK, Choi SS, Bradrick S, Karaca GF, et al. Viral factors induce Hedgehog pathway activation in humans with viral hepatitis, cirrhosis, and hepatocellular carcinoma. *Lab Invest* 2010;90:1690–703.
18. Jung Y, McCall SJ, Li YX, Diehl AM. Bile ductules and stromal cells express hedgehog ligands and/or hedgehog target genes in primary biliary cirrhosis. *Hepatology* 2007;45:1091–6.
19. Chen X, Lingala S, Khoobyari S, Nolte J, Zern MA, Wu J. Epithelial mesenchymal transition and hedgehog signaling activation are associated with chemoresistance and invasion of hepatoma subpopulations. *J Hepatol* 2011;55:838–45.
20. Chen XL, Cao LQ, She MR, Wang Q, Huang XH, Fu XH. Gli-1 siRNA induced apoptosis in Huh7 cells. *World J Gastroenterol* 2008;14:582–9.
21. Chen XL, Cheng QY, She MR, Wang Q, Huang XH, Cao LQ, et al. Expression of sonic hedgehog signaling components in hepatocellular carcinoma and cyclopamine-induced apoptosis through Bcl-2 down-regulation *in vitro*. *Arch Med Res* 2010;41:315–23.
22. Chen YJ, Lin CP, Hsu ML, Shieh HR, Chao NK, Chao KS. Sonic hedgehog signaling protects human hepatocellular carcinoma cells against ionizing radiation in an autocrine manner. *Int J Radiat Oncol Biol Phys* 2011;80:851–9.
23. Cheng WT, Xu K, Tian DY, Zhang ZG, Liu LJ, Chen Y. Role of Hedgehog signaling pathway in proliferation and invasiveness of hepatocellular carcinoma cells. *Int J Oncol* 2009;34:829–36.
24. Huang S, He J, Zhang X, Bian Y, Yang L, Xie G, et al. Activation of the hedgehog pathway in human hepatocellular carcinomas. *Carcinogenesis* 2006;27:1334–40.
25. Patil MA, Zhang J, Ho C, Cheung ST, Fan ST, Chen X. Hedgehog signaling in human hepatocellular carcinoma. *Cancer Biol Ther* 2006;5:111–7.
26. Sicklick JK, Li YX, Jayaraman A, Kannangai R, Qi Y, Vivekanandan P, et al. Dysregulation of the Hedgehog pathway in human hepatocarcinogenesis. *Carcinogenesis* 2006;27:748–57.
27. Bisht S, Brossart P, Maitra A, Feldmann G. Agents targeting the Hedgehog pathway for pancreatic cancer treatment. *Curr Opin Investig Drugs* 2010;11:1387–98.
28. Buonamici S, Williams J, Morrissey M, Wang A, Guo R, Vattay A, et al. Interfering with resistance to smoothed antagonists by inhibition of the PI3K pathway in medulloblastoma. *Sci Transl Med* 2010;2:51ra70.
29. Dijkgraaf GJ, Aliche B, Weinmann L, Januario T, West K, Modrusan Z, et al. Small molecule inhibition of GDC-0449 refractory smoothed mutants and downstream mechanisms of drug resistance. *Cancer Res* 2011;71:435–44.
30. Yauch RL, Dijkgraaf GJ, Aliche B, Januario T, Ahn CP, Holcomb T, et al. Smoothed mutation confers resistance to a hedgehog pathway inhibitor in medulloblastoma. *Science* 2009;326:572–4.
31. Hoshida Y, Toffanin S, Lachenmayer A, Villanueva A, Minguez B, Llovet JM. Molecular classification and novel targets in hepatocellular carcinoma: recent advancements. *Semin Liver Dis* 2010;30:35–51.
32. Nolan-Stevaux O, Lau J, Truitt ML, Chu GC, Hebrok M, Fernández-Zapico ME, et al. GLI1 is regulated through Smoothed-independent mechanisms in neoplastic pancreatic ducts and mediates PDAC cell survival and transformation. *Genes Dev* 2009;23:24–36.
33. Hyman JM, Firestone AJ, Heine VM, Zhao Y, Ocasio CA, Han K, et al. Small-molecule inhibitors reveal multiple strategies for Hedgehog pathway blockade. *Proc Natl Acad Sci U S A* 2009;106:14132–7.
34. Chenna V, Hu C, Pramanik D, Aftab BT, Karikari C, Campbell NR, et al. A polymeric nanoparticle encapsulated small molecule inhibitor of hedgehog signaling (NanoHHL) bypasses secondary mutational resistance to smoothed antagonists. *Mol Cancer Ther* 2012;11:165–73.
35. Ishak KG, Anthony PP, Sobin LH. Nonepithelial tumors. In: Ishak KG editor. *Histological typing of tumors of the liver*. (World Health Organization International Classification of Tumors). 2nd ed. Berlin: Springer; 1994. p. 22–7.
36. Poon RT, Ng IO, Lau C, Yu WC, Yang ZF, Fan ST, et al. Tumor microvessel density as a predictor of recurrence after resection of hepatocellular carcinoma: a prospective study. *J Clin Oncol* 2002;20:1775–85.
37. Wittekind C. Pitfalls in the classification of liver tumors. *Pathologie* 2006;27:289–93.
38. Gao Q, Qiu SJ, Fan J, Zhou J, Wang XY, Xiao YS, et al. Intratumoral balance of regulatory and cytotoxic T cells is associated with prognosis of hepatocellular carcinoma after resection. *J Clin Oncol* 2007;25:2586–93.
39. Cai XY, Gao Q, Qiu SJ, Ye SL, Wu ZQ, Fan J, et al. Dendritic cell infiltration and prognosis of human hepatocellular carcinoma. *J Cancer Res Clin Oncol* 2006;132:293–301.
40. Fu X, Wang Q, Chen X, Huang X, Cao L, Tan H, et al. Expression patterns and polymorphisms of PTCH in Chinese hepatocellular carcinoma patients. *Exp Mol Pathol* 2008;84:195–9.
41. Lingala S, Cui YY, Chen X, Ruebner BH, Qian XF, Zern MA, et al. Immunohistochemical staining of cancer stem cell markers in hepatocellular carcinoma. *Exp Mol Pathol* 2010;89:27–35.
42. Oliva J, French BA, Qing X, French SW. The identification of stem cells in human liver diseases and hepatocellular carcinoma. *Exp Mol Pathol* 2010;88:331–40.
43. Vroiling L, Lind JS, de Haas RR, Verheul HM, van Hinsbergh VW, Broxterman HJ, et al. CD133+ circulating haematopoietic progenitor cells predict for response to sorafenib plus erlotinib in non-small cell lung cancer patients. *Br J Cancer* 2010;102:268–75.
44. Imamura H, Matsuyama Y, Tanaka E, Ohkubo T, Hasegawa K, Miyagawa S, et al. Risk factors contributing to early and late phase

- intrahepatic recurrence of hepatocellular carcinoma after hepatectomy. *J Hepatol* 2003;38:200–7.
45. Coulouarn C, Factor VM, Thorgeirsson SS. Transforming growth factor-beta gene expression signature in mouse hepatocytes predicts clinical outcome in human cancer. *Hepatology* 2008;47:2059–67.
46. Feng YX, Wang T, Deng YZ, Yang P, Li JJ, Guan DX, et al. Sorafenib suppresses postsurgical recurrence and metastasis of hepatocellular carcinoma in an orthotopic mouse model. *Hepatology* 2011;53:483–92.
47. Ma S, Chan KW, Hu L, Lee TK, Wo JY, Ng IO, et al. Identification and characterization of tumorigenic liver cancer stem/progenitor cells. *Gastroenterology* 2007;132:2542–56.